Acta Cryst. (1997). A53, 84–94

Side-Face Structure and Growth Mechanism of Tabular Silver Bromide Crystals

G. Bögels,[a] T. M. Pot,[a] H. Meekes,[a]* P. Bennema[a] and D. Bollen[b]

[a]*RIM Laboratory for Solid State Chemistry, University of Nijmegen, Toernooiveld, 6525 ED Nijmegen, The Netherlands, and* [b]*Agfa-Gevaert NV, Septestraat 27, B-2640 Mortsel, Belgium. E-mail: hugom@sci.kun.nl*

(*Received 12 July 1996; accepted 4 October 1996*)

Abstract

Recently, it has become possible to grow large tabular silver bromide crystals from organic solvents, which makes direct observation of the side faces possible. Solving the side-face structure is a key to understanding the (lateral) growth mechanism of tabular silver bromide crystals. The side-face structure of 42 tabular crystals was determined in detail. The side-face structure of the tabular crystals is built up by flat {111} and {100} cubo-octahedral faces and there are three different kinds of tabular morphology. In all observations, ridge structures were found showing no acute lips. From these determinations, the number of parallel twin planes of the tabular crystals was directly reduced from the side-face structure. The lateral growth of the tabular crystals is described by a substep mechanism. This mechanism explains the increase of growth rate of a {111} side face that is linked with a twin plane to a {100} side face. The proposed substep mechanism is based on a theory of Ming, which is universal and not only valid for the case of silver bromide. The interpretation assumes the presence of only cubo-octahedral faces and the absence of acute lips as observed.

1. Introduction

For several decades, there has been interest in the growth mechanism of tabular silver bromide crystals. Around the surface of these crystals, the photographic process takes place. Tabular crystals have a relatively large surface and, consequently, with spectrally sensitized emulsions less silver is needed compared with block-shaped crystals. Large amounts of tabular crystals are produced in the photographic industry under well defined conditions. However, there are still many questions concerning the conditions under which the growth of tabular crystals takes place. The side-face geometry of tabular crystals is not completely understood. One of the problems in solving the side-face structure is the size of the crystals. Under normal precipitation conditions in aqueous solution, in which the emulsion for practical use is formed, the maximum size of the crystals is a few micrometres. These small crystals have prohibited an elucidation of the growth mechanism involved. Recently, it turned out to be also possible to grow large tabular crystals from organic solvents (Millan & Bennema, 1997). The solubility of silver halide in Me_2SO is so high that tabular crystals can grow up to 1 cm. The advantage of this size is that the side-face structure of these tabular crystals can be carefully examined. Solving the side-face structure is a key to understanding the growth mechanism of silver bromide tabular crystals.

The first crystal models to explain the morphology of tabular crystals were based on the assumption that these crystals were bounded by {111} faces (Berriman & Herz, 1957; Hamilton & Brady, 1964; Klein, Metz & Moisar, 1963; Sugimoto, 1984; Maskasky, 1987*a*). Tabular crystals are accordingly formed from octahedral seed crystals with twin planes parallel to the (111) surface. The side-face structure was believed to have ridges and troughs, the latter serving as re-entrant grooves. Berriman & Herz (1957) found, using Laue photography, that most tabular crystals have twin planes parallel to the large (111) face. Twin planes were according to them not only formed during the nucleation stage but also during the subsequent growth of the crystal. The lateral growth of the crystals was explained as being due to the troughs on the sides facilitating nucleation for deposition of successive ionic layers relative to the flat structures of the big tabular faces.

Hamilton & Brady (1964) studied 56 tabular crystals with different kinds of replica technique. From these crystals, 53 showed an even number and 3 an odd number of twin planes. When the crystals were given a latent-image exposure, it was also possible to reveal the distances between the twin planes as 0.04 μm for a crystal of 0.4 μm thickness. They speculated that, once the rapid growth resulting from the twinned structure begins, the local supersaturation of the constituent ions would decrease in the immediate neighbourhood of the grain. Perhaps this would reduce the probability of forming additional twins.

With scanning electron microscopy (SEM), the side-face structure was revealed (Hamilton & Brady, 1958; Farnell & Judd, 1961; Klein, Metz & Moisar, 1963). Tabular crystals were tilted so that their side-face geometry became visible with SEM. Two studies

(Farnell & Judd, 1961; Klein, Metz & Moisar, 1963) presented crystals with two side faces in a ridge geometry.

Sugimoto (1984) questioned the importance of the re-entrant grooves as a favourite site for nucleation. He discussed the possibility of crystallographic planes being present on the sides of tabular crystals. Maskasky (1987*a*) suggested that an acute lip on the crystal side face was the preferred place for nucleation. An experimental study on tabular crystals revealed that most triangularly shaped crystals had an odd number of parallel twin planes and most regular hexagons and truncated triangular crystals had an even number. Maskasky (1987*b*) later invented a new method for determining the separation between the parallel twin planes. He added a growth modifier that inhibits lateral growth of the obtuse region of the tabular crystal structure while allowing limited lateral growth on the remaining edge structure. The observed distances were in good agreement with the measurements done by Hamilton & Brady (1964). This proved again that twinning occurred at the nucleation stage. However, they did not find evidence to suggest that octahedra can serve as seeds for tabular crystals. Mehta, Jagannathan & Timmons (1993) proposed a model where the side-face structure consists of cubo-octahedral faces ({111} and {100} faces). The seed crystals for tabular growth were believed to be cubo-octahedrons instead of octahedrons. Jagannathan, Mehta, Timmons & Black (1993) used the Hamilton & Seidersticker model to explain the lateral growth. A mechanism was proposed where the self-regeneration of the side faces is driven by {100} planes in twinned contact with the acute {111} planes. The starting side-face structure consists of a ridge–trough structure built up by {111} faces. Owing to the high probability of adatoms to incorporate at the re-entrant grooves, the growth will be initiated there by stable clusters. The growth layer will be initiated from a re-entrant groove that extends in two opposite directions. When the growth layer approaches the ridge, a vicinal {100} face emerges. van der Waal (1995) criticized the application of the model of Hamilton & Seidersticker to explain the lateral growth because this model was used for ionic crystals. Mehta, Jagannathan, Lam, Black & Timmons (1995) examined the number of twin planes for the different shapes of tabular crystals. They found no correlation between the shape of the crystal and the number of twin planes as had been suggested by Maskasky (1987*a*). The earlier proposed cubo-octahedron model (Mehta, Jagannathan & Timmons, 1993) gives, according to them, a reasonable explanation for the difference in the shape of tabular crystals with two twin planes. However, the authors' opinion was that additional techniques must be sought to determine the side-face structure of tabular crystals. Recently, Mehta, Jagannathan & Timmons (1996) suggested for tabular crystals with three parallel twin planes that the {100}/{111} rough–smooth structure could develop during the process of preparation. According to them, some of the side-face structures were transformed from {111} bounded structures to {100} bounded structures during the process of preparation. However, one rough–smooth structure was still expected to develop during the precipitation.

In this paper, we shall reveal the side-face structure of tabular silver bromide crystals. No new techniques were used, only the size of the crystals was enlarged in such way that 'old' techniques were accurate enough to solve the structure. Also, it was possible to remove the crystals from the mother liquid without inducing growth effects on the surface.

The side-face structure is a powerful tool for explaining the growth history of tabular crystals. We were able to find a relation between the number of twin planes present in a crystal and a specific side-face structure. Also, a model is presented that explains the lateral growth. This model is based on the theory of Ming (Ming & Sunagawa, 1988; Ming & Li, 1991; Ming 1993), who performed an important study on the growth mechanism of twinned f.c.c. crystals.

2. Experimental

2.1. *Preparation of the tabular crystals*

A solution (I) was prepared by dissolving 9.39 g of silver bromide and 5.95 g of potassium bromide in 50 ml of Me_2SO. Another solution (II) was prepared by mixing 2 ml of water with 4 ml of Me_2SO. To solution (I), solution (II) was added dropwise while stirring until a precipitate was formed. The stirring was thereafter stopped and the mixture was kept in the dark for one month. The crystals thus grew to a size of 2–10 mm in a physical ripening process. The aspect ratio (diameter of the large {111} top faces divided by the thickness of the crystal) of the examined crystals ranged from 4 to 60. The crystals were carefully taken out of the mother liquid in order not to damage the side-face structure and placed immediately in pure Me_2SO for a short time to prevent precipitation of silver bromide or potassium bromide on the crystal surface. This process must be handled with extreme care to avoid roughening of the side faces. For crystals with an aspect ratio above 100, we were unable to avoid roughening. These crystals also bent when standing perpendicular to the tabular faces. This makes it impossible to identify the side faces.

2.2. *Examination of the tabular crystals*

When the crystals were taken out of the mother liquid, they were examined with an optical goniometer. With such a goniometer, one is able to measure the angles between the different faces of a crystal with an accuracy of $\pm 20'$. The large top and bottom faces [(111)

and $(\bar{1}\bar{1}\bar{1})$] of the tabular crystal were taken as reference faces. The angles of the side faces were measured with respect to the chosen reference faces. The results were included in a stereographic projection and indexed to (*hkl*) faces. While tabular crystals have twin planes parallel to a {111} face, they contain side-face orientations that are not present in single crystals. For those 'twin faces', a prime was added in the indexing ({*hkl*}').

The side-face structure is still too small to be observed directly on the goniometer. So the next step was to examine the side-face profile with a SEM (JEOL JSM-6310) to find the correct order of the indexed faces of the side-face structure. At the same time, the indexed face orientations were roughly remeasured. The profile was important to make a distinction between the different side-face geometries possible with the indexed faces. The samples were placed on their side faces in order to be able to study the orientations of the side-face structure in detail. The crystals were gold sputtered.

3. Results

3.1. *Group 1 tabular crystals*

We found three different morphologies for the tabular crystals. Therefore, they were divided into three groups. Group 1 tabular crystals have shapes ranging from a perfect hexagon to hexagons with a ratio of long-edge dimension to short-edge dimension of 8:1. About 76% of the examined crystals belong to this group. The side-face structure consists of two adjacent faces in a ridge structure (visualized in Fig. 1). Between these faces, there is a small area where the twin plane(s) are expected to be located. The crystal side 1 consists of adjacent flat {100} and flat {111} faces. The angle between the top face and the {100} side face is 125°16′. Between the {111} and the bottom face, the angle is 109°29′. The crystal sides 1′ and 1″ have a side-face geometry equivalent to that of 1. The neighbouring crystal sides (2, 2′ and 2″) also have a flat {111} and a flat {100} face in reverse order.

The side-face structure is visualized by tilting the crystals in the SEM perpendicular to the large tabular faces. In Fig. 2, an example of such a side-face structure can be seen.

3.2. *Group 2 tabular crystals*

Group 2 crystals express a different number of side faces compared with group 1. They have shapes ranging from a perfect triangle to hexagonals with a ratio of long-edge dimension to short-edge dimension of 3:1. Thus, there is an overlap in the definition of group 2 and group 1. The side-face structure consists also of {111} and {100} faces. The difference between the group 1 tabular crystals (Fig. 1*a*) and the group 2 tabular crystal (Fig. 1*b*) is the number and the order of the side faces. Group 2 crystals have a different side-face structure for the long and short crystal sides. On the long side, there are two {111} side faces adjacent to the tabular faces with a {100} face in between in a ridge/trough structure, as visualized in Fig. 1(*b*). The short sides (if visible) consist of two {100} faces with a {111} face between, resulting in a ridge structure. The side-face

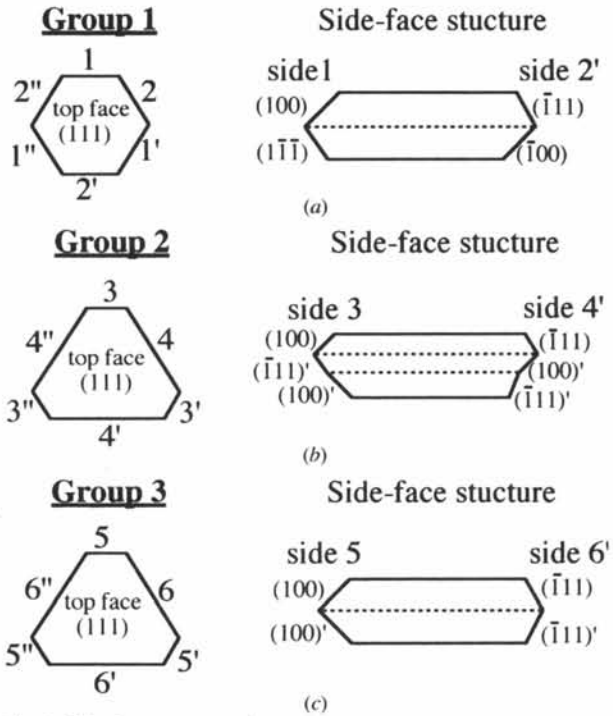

Fig. 1. Side-face structure of: (*a*) group 1 tabular crystals; (*b*) group 2 tabular crystals; and (*c*) group 3 tabular crystals. The dashed line in the tabular crystals is the area where the twin planes are expected to be located. The actual number of twin planes in each area will become clear in the following. The primes refer to twin faces that do not appear on single crystals.

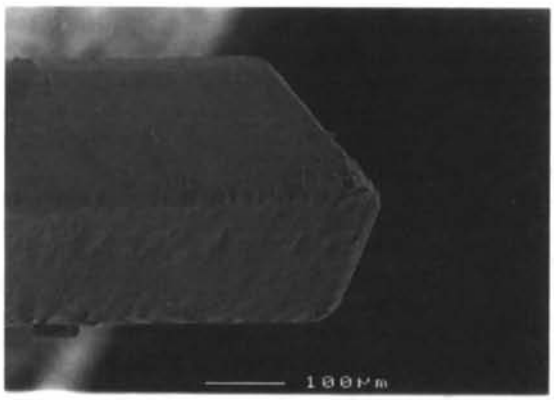

Fig. 2. SEM image of the side-face structure of a tabular crystal of group 1. The {111} top face is oriented horizontally. The side-face geometry is the same as in Fig. 1(*a*), side 1.

structure of the long side of a tabular crystal of group 2 is visualized in Fig. 3.

3.3. *Group 3 tabular crystals*

Group 3 crystals have the same shape as those of group 2 but express a different number of side faces. They have again a different side-face geometry for the long and short crystal sides (Fig. 1*c*). On the long sides, there are two adjacent {111} faces in a ridge structure. The short side (if visible) consists of two adjacent {100} faces. This side-face geometry is visualized in Fig. 4. It is concluded that the tabular crystals of groups 2 and 3 have the same side faces adjacent to the tabular faces.

The side-face structure determination discussed above has been carried out for 42 tabular crystals. All these crystals were examined with the goniometer and SEM. The results are summarized in Table 1, which illustrates that 41 of the 42 examined crystals showed a well defined side-face geometry. This is an improvement compared with TEM measurements done on 'little' tabular crystals (Jagannathan, Mehta, Timmons & Black, 1993). All the 41 crystals with a well defined side-face geometry could be classified into one of our crystal groups.

Table 1. *Tabular crystals examined*

	Amount	Crystals with an anomalous face*	Crystals with two anomalous faces	Not all side faces were measured†
Group 1	32 (76.2%)	1	1	3
Group 2	4 (9.5%)	–	–	1
Group 3	5 (11.9%)	1	–	1
Other tabular crystals	1 (2.4%)	–	–	–

*An anomalous face is a {111} face where a {100} face would be expected or *vice versa*. †For some crystals, we were not able to measure all side faces without damaging or bending the crystal. This does not mean there were no side faces, but owing to the high aspect ratio (between 40 and 60) of the crystals we were unable to measure them all.

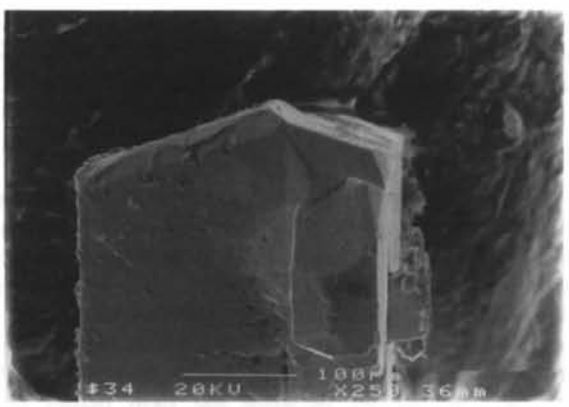

Fig. 3. SEM image of the side-face structure of the long side of a tabular crystal of group 2. The {111} top face is oriented vertically. The side-face geometry is the same as in Fig. 1(*b*), side 4′.

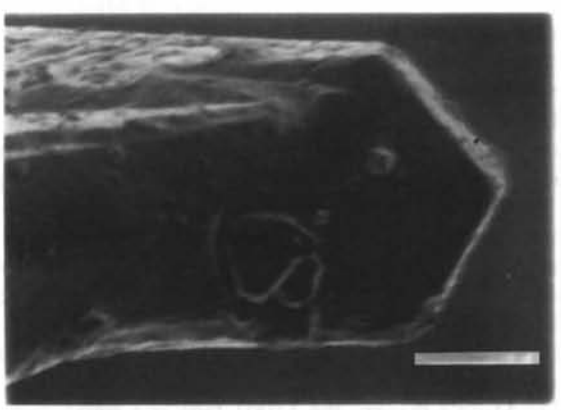

Fig. 4. SEM image of the side-face structure of the short side of a tabular crystal of group 3. The {111} top face is oriented horizontally. The side-face geometry is the same as in Fig. 1(*c*), side 5. The white bar is 100 µm.

4. Discussion

4.1. *Number of twin planes*

The observed side-face geometries of the different tabular crystal groups are made up entirely of cubo-octahedral faces. The morphology of the crystals of group 1 can be constructed from the side-face structure of Fig. 1(*a*). This gives a crystal that can be considered as a flat cubo-octahedron when we neglect the details in the neighbourhood of the twin planes. Recently, some models were proposed to clarify the shape of the seed crystals (Maskasky 1987*a*; Mehta, Jagannathan & Timmons, 1993). In these models, the purely {111}-bound side-face geometry was more and more changed into a shape with cubo-octahedral faces. However, there are still some doubts whether the equilibrium habit of the cubo-octahedron is already developed under the high supersaturation (where twinning takes place) in a reactor (Mehta, Jagannathan, Lam, Black & Timmons, 1995).

In our model, we do not assume the cubo-octahedron to be the equilibrium form of the seed crystal. In fact, the seed crystal can be an octahedron, a cubo-octahedron or even a rough rounded octahedron or cubo-octahedron. It is assumed that parallel twinning occurs in the nucleation stage and, therefore, the distances between the twin planes are very small ($\ll 1\,\mu m$). In a later stage of the precipitation, the cubo-octahedron becomes the stable growth form. The twin planes present, then, induce the growth of the tabular crystals.

We distinguish between nucleation twin planes, which are formed in the early nucleation stage, and therefore close together, and accidental twin planes, which are due to accidental twinning in a later stage or

to coalescence. From our classification, we are able to establish the number of twin planes for the different crystal groups.

4.1.1. *Single twinning*. A nucleation twin plane in a cubo-octahedron can be considered as a rotation of the top with regard to the bottom of the crystal by 60°. This rotation (or single twinning) is visualized in Fig. 5. The idea that a twin plane can be considered as a rotation was also made by Mitchell (1957). The physical relevance of such a twin will be discussed in the section concerning lateral growth.

The side-face geometry of the single twinned crystal in Fig. 5 has the same geometry as that of the tabular crystals of group 3. However, we shall see that single twinned crystals do not express preferential lateral growth.

4.1.2. *Double twinning*. Adding another nucleation twin plane gives a side-face geometry (again neglecting the structure between the twin planes) of a (flat) cubo-octahedron. The tabular crystals of group 1 have such a side-face structure (see Figs. 1 and 5). In general, an even number of nucleation twin planes gives rise to tabular crystals of group 1.

4.1.3. *Triple twinning*. A third nucleation twin plane gives again the side-face structure (neglecting the structure between the twin planes) of the tabular crystals of group 3 [Figs. 1(*c*) and 5, triple twinning (2)]. In general, group 3 crystals have an odd number of nucleation twin planes, but have at least three. When adding to the group 1 crystals an accidental twin plane, we get a crystal with the same side-face geometry as the tabular crystals of group 2 [Figs. 1(*b*) and 5, triple twinning (1)]. Therefore, we can conclude that for the tabular crystals of group 1 the number of twin planes is two and for groups 2 and 3 the number of twin planes is three. Combined with the results presented in Table 1, it means that about 76% of the crystals have two (or an even number of) twin planes and about 21% of the crystals have three (or an odd number of) twin planes. If we assume that growth of silver bromide crystals in MeSO, as far as the morphology is concerned, is in principle comparable with that in water, given the polar character of both solvents, we can compare our results with those of others. Our results are in reasonable agreement with the work of Hamilton & Brady (1964) and Maskasky (1987*a*). The former found about 95% of the tabular crystals with two twin planes and 5% with three twin planes in water. Maskasky established also in water that about 90% of his total population had an even number and 6.5% an odd number of twin planes, which again is in reasonable agreement with our results.

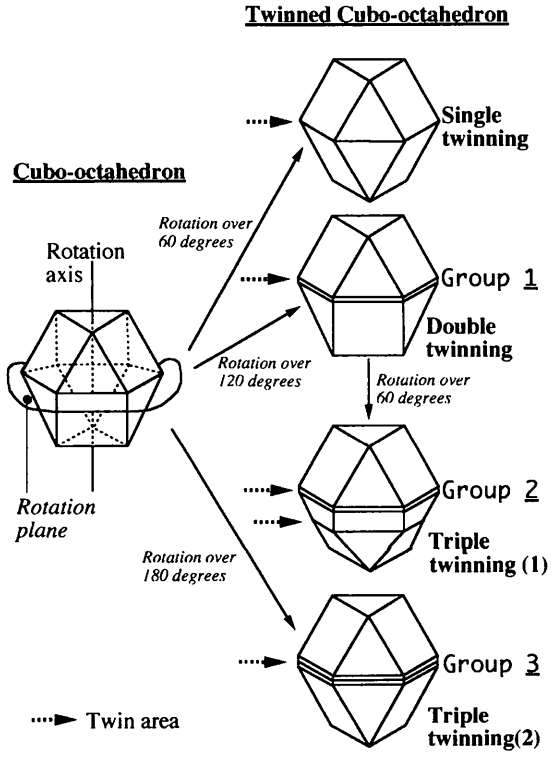

Fig. 5. Morphologies resulting from different numbers of twin planes. The rectangular faces are the {100} faces; the others are the {111} faces.

4.2. *Lateral growth mechanism*

For the tabular silver bromide crystals, we have identified the adjacent side faces present for the three groups of observed crystals. With the twinned cubo-octahedron model, we have deduced the number of twin planes of the three crystal groups. In this section, a mechanism is discussed for the preferential lateral growth of the tabular crystals. We deduce the possible side-face geometries between the twin planes on a microscopic level and the contribution of these faces to the lateral growth using a recently developed model for crystal growth.

The model is based on the theory of Ming (Ming & Sunagawa, 1988; Ming & Li, 1991; Ming, 1993), who explained the preferential lateral growth of f.c.c. crystals with twin planes and stacking faults by means of substeps. A twin plane between two crystal faces can introduce a substep that serves as a step source for both faces. These steps are continuously present, resulting in a continuous step source, somewhat analogous to the spiral growth mechanism discussed by Frank (1949). In the model, only the nearest-neighbour interactions were taken into account. It is assumed that the most likely place for the adatom to incorporate on the surface is the place where it has a maximum number of nearest neighbours.

In Ming's theory, the {100} face is a rough face. In the case of silver bromide, we observe flat {100} faces. Therefore, we will expand this theory for crystals with flat {100} and {111} faces. We will see with our model

that between {100} and {111} faces substeps can emerge with a height of 2/3 or 1 of the interplanar distance d_{111}.

The lateral growth model is visualized by a sphere model representing one kind of ion or rather a complete AgBr entity, which we loosely call an atom. In the following, we will closely examine the growth rate of the {100} faces in comparison with the {111} faces. We assume that the {100} faces are growing faster than the {111} faces because the number of neighbours for adatoms on a {100} face is higher than on a {111} face. An adatom on a {100} surface has four neighbouring atoms and on a {111} face it has three. Therefore, we assume that the incorporation of an adatom on a {100} face is more likely to occur. A second adatom on a {100} surface connected to the first one has five neighbours whereas on a {111} face it will have only four. So a critical two-dimensional nucleus is more easily formed on a {100} face, resulting in a higher growth rate. We also assume that the formation of a critical two-dimensional nucleus is the rate-determining step in the growth process. As soon as such a nucleus has formed, the new growth layer will be formed.

Here we neglect the effect of the polar character of the {111} faces as compared to the dipoles parallel to the {100} faces. Thus, the main assumptions in our model for the growth mechanism are:

(*a*) The growths units are silver bromide molecules represented by spheres;

(*b*) {111} and {100} faces grow as flat faces;

(*c*) {100} faces grow faster than {111} faces, in other words, two-dimensional nucleation occurs more easily on a {100} face;

(*d*) larger faces have a larger chance of forming a two-dimensional nucleus.

4.2.1. *Single crystals.* We start with a flat single crystal of a cubo-octahedron as discussed in the previous section. In Fig. 6, a cut perpendicular to the large tabular (top) face and through the middle of two opposite crystal sides, for example 1 and 2′ (Fig. 1), is made. In Fig. 6, only two of the six crystal sides are visible. The other side faces are of course equivalent. We will discuss the effect a twin plane has on the growth rate for the three different crystal groups.

4.2.2. *Substeps.* In Fig. 7, the possible side-face structures of a single twin plane present in a {100} or {111} side face are drawn. We assume that only cubo-octahedron faces are the stable ones in the later stage of the precipitation and during the physical ripening. Furthermore, we do not consider acute edges on side faces adjacent to the tabular faces because we found that these side faces of tabular silver bromide crystals are always obtuse. Two types (*a* and *b*) are more closely examined. In Fig. 8(*a*), the geometries of Figs. 7(*a*) and (*b*) are drawn within the sphere model. On the left-hand side of Fig. 8(*a*), a {100} face is going over in a {111} face owing to the twin plane (dashed line) corresponding to the case of Fig. 7(*a*). On the right-hand side of Fig. 8(*a*), the {111} face is changed to a {100} face owing to the twin plane, corresponding to the case of Fig. 7(*b*).

When the crystal of Fig. 8 is placed in a supersaturated environment, two-dimensional nucleation is expected to occur on the (100) face. In this case, a new growth layer will be formed on the (100) surfaces (Fig. 8*b*). The atoms near the twin planes are placed in such a way that the last atom near the {111} faces has a perfect {100} surrounding.

On the left-hand side of the crystal, a substep of height 2/3 of d_{111} is formed (Fig. 8*b*). In this substep position, adatoms can more easily be accommodated. With a three-dimensional model, one is able to visualize the number of neighbouring atoms available for the adatom placed in this substep position. An isolated adatom of a surface site on a {111} plane has three nearest neighbours whereas an atom placed in the substep has four neighbours (Fig. 8*c*). In the crystal on the right-hand side of Fig. 8, a substep is also formed. The height of the substep is d_{111}. Adatoms incorporated at that position will have five instead of three neighbouring atoms (see Fig. 8*c*).

After these atoms are incorporated, normal steps (corresponding to five neighbouring atoms in the step) and kink sites (six neighbours) are easily introduced on both (111) faces. These steps and kink sites increase the growth rate on the (111) faces and soon a new growth layer will be formed (Fig. 8*d*). The growth will be continued by nucleation on the (100) faces and so on.

It is assumed that the rate-determining step for the profiles is the place where an adatom has the smallest number of neighbours. For the substep of 2/3, the rate-determining step is the incorporation of an adatom on a {100} face to form a critical nucleus and the incorporation in the substep position. For the substep

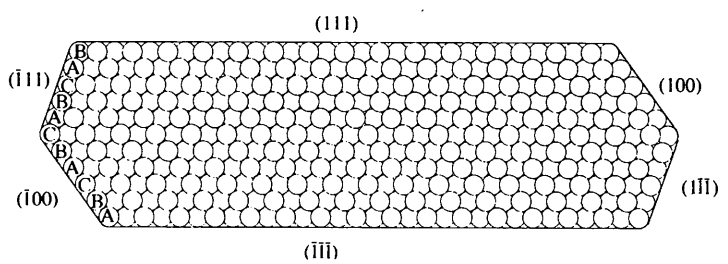

Fig. 6. Microscopic cross section of a flat single cubo-octahedron crystal made up of spheres.

of height d_{111}, the rate-determining step is only the two-dimensional nucleation on the {100} face. Therefore, it is assumed that the substep of 1 has a somewhat higher growth rate than the substep of 2/3. It is concluded that twin planes introduce two different types of substep that increase the growth rate of the (111) faces.

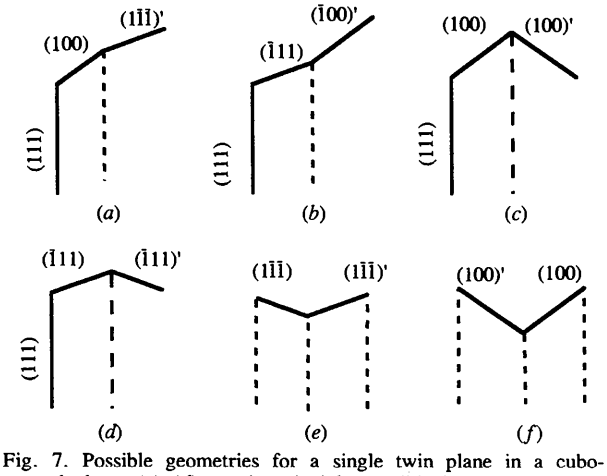

Fig. 7. Possible geometries for a single twin plane in a cubo-octahedron. (*a*)–(*f*) are in principle possible between two twin planes, (*a*)–(*d*) only possible adjacent to a tabular face (vertical solid lines). The twin lines are the dashed lines.

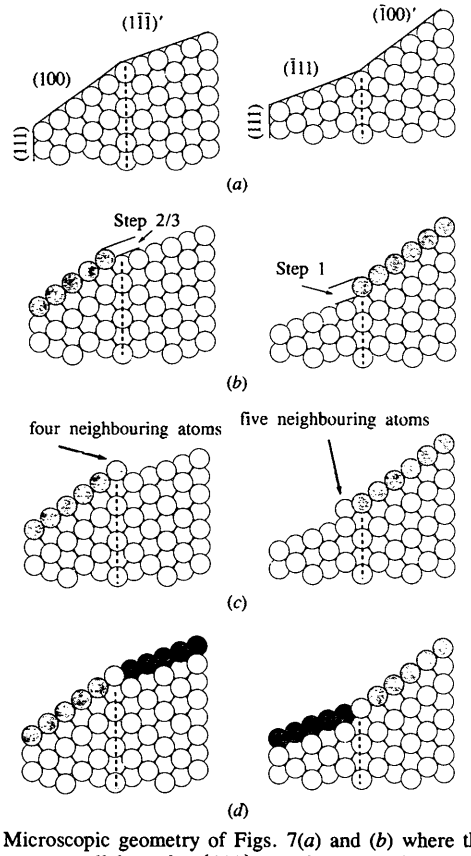

Fig. 8. Microscopic geometry of Figs. 7(*a*) and (*b*) where the twin planes are parallel to the {111} top face (not drawn). (*a*)–(*d*) correspond to different stages of the substep-induced growth mechanism.

Returning to Fig. 7, we found that for the side-face geometries of Figs. 7(*c*)–(*f*) no substeps are present. The growth rate of the profile in Fig. 7(*c*) is determined by the growth rate of the {100} faces and for the geometry in Fig. 7(*d*) it is determined by the growth rate of the {111} faces. On sides shown in Figs. 7(*e*) and (*f*), an adatom incorporates most easily between the two faces in the re-entrant corner. For the profile in Fig. 7(*e*), it will have four neighbouring atoms, for that in Fig. 7(*f*), it will have six. After these atoms are built in, normal steps on both faces can easily be formed. The rate-determining step for these profiles is somewhat smaller than for Figs. 7(*a*) and (*b*) because two-dimensional nucleation can only occur in the re-entrant groove and not on a whole plane.

Comparing all possible situations of Fig. 7, we conclude that Fig. 7(*f*) shows the fastest growing side (only one row provides six neighbouring atoms) followed by Figs. 7(*b*) and (*c*) (with four neighbouring atoms on a {100} face) then Fig. 7(*a*) (with four neighbouring atoms on a {100} face and in the substep position), Fig. 7(*e*) (only one row provides four neighbouring atoms) and last Fig. 7(*d*) (three neighbouring atoms on a {111} face).

We will use these differences in growth rates to interpret the different kinds of side-face structure on tabular crystals.

4.2.3. *Single twinning.* When in the flat cubo-octahedron crystal one twin plane is present (Fig. 9), one crystal side will contain two {100} faces, corresponding to Fig. 7(*c*), whereas the other crystal side will contain two {111} faces, corresponding to Fig. 7(*d*). On both crystal sides, no substep mechanism will be expressed. Therefore, the growth rate of the {100} crystal side will be higher than the {111} side. Thus, the {100} sides will be able to grow out of the crystal leaving a triangularly shaped crystal behind. This triangular single twinned crystal will be built up entirely by {111} faces expressing no preferential lateral growth. Such shapes have been observed by Millan & Bennema (1997) a short time after precipitation in Me_2SO. We did not observe these shapes. This was probably because we left the crystal to grow for one month. Because these single twinned crystals did not express preferential lateral growth, they might dissolve in the physical ripening process after precipitation. This led us to the conclusion that tabular crystals always have at least two nucleation twin planes.

In the following section, we will discuss the relevance of the twin planes that induce preferential lateral growth for the three groups of crystals observed.

4.2.4. *Lateral growth of group 1 crystals (double twinning).* Two twin planes in the flat cubo-octahedron give rise to the tabular crystals that can have only two different side-face geometries as depicted in Fig. 1(*a*)

because for these crystals the side faces adjacent to the top and bottom faces are always obtuse. Crystals of group 1, therefore, are made up of these two side-face structures and their inversion images, resulting in three different possible crystal morphologies, assuming that the threefold symmetry is conserved.

Crystal side *A* (Fig. 10) consists of two {100} faces and one {111} face. As already discussed, the growth rate is determined by the two-dimensional nucleation on both {100} faces and on the substep position. On this position, a substep of height d_{111} will be formed that is able to increase the growth rate on the {111} face (the same as Fig. 7*b*). The growth rate for crystal side *B* will be determined by the two-dimensional nucleation on the (100) face. Again, a substep will be formed on the $(1\bar{1}\bar{1})'$ face between the twin planes (the same as Fig. 7*a*). On this {111} face, normal step and kink sites will be formed. When this step reaches the end of this face, it facilitates a preferential site for the $(1\bar{1}\bar{1})$ face owing to the presence of a vicinal {100} face. An adatom adsorbed on this place will have four neighbours. So the growth rate on this face will also increase owing to the substep mechanism. It is clear that both side-face structures express preferential lateral growth owing to the substep mechanism. However, it is difficult to deduce from this simple model the growth rate of the different sides. We assume that the growth rate of side *A* is somewhat different from side *B* because for both sides different substep mechanisms are active.

Therefore, group 1 crystals consist of three kinds of morphology. Crystals with all crystal sides either *A* or *B* and crystals with three *A* and three *B* sides. This implies that tabular crystals with two twin planes are regular hexagons (all crystal sides have either profile *A* or profile *B*) or more intermediate shapes (crystals with three *A* and three *B* sides). This is in agreement with our observations and also explains the occurrence of more triangular shaped crystals with two twin planes.

4.2.5. *Lateral growth of group 2 and group 3 crystals (triple twinning).* The presence of three twin planes in a cubo-octahedron leads to crystals with the side-face structure of the tabular crystals of groups 2 and 3 (see Figs. 1*b*, *c* and 5). There are six different side-face structures possible, again neglecting the inversion images. Three of these structures are possible for the short crystal sides, which can be seen in Fig. 11 (sides *C*, *D* and *E*). Crystal side *E* will express preferential lateral growth because it is completely built up by {100} faces. Adatoms will preferentially incorporate in the re-entrant corner because they will have six neighbouring atoms. This incorporation increases the growth rate of the {100} faces between the twin planes over the {100} faces adjacent to the tabular faces that are growing only by two-dimensional nucleation. When this happens, these {100} faces will grow out of the crystal leaving {111} faces behind, resulting in side *C*. Side-face structure *E* was also proposed by Mehta, Jagannathan & Timmons (1993). They believed that this side occurs on hexagonal tabular crystals. However, we observed it on more triangular-shaped tabular crystals. Side *C* will also express preferential lateral growth while the two {111} faces are linked with substeps to the {100} faces. Crystal side *D* contains one {111} face, which is linked by two substeps. Thus, this side will also express preferential lateral growth. The growth rate of sides *C* and *D* are expected to be more or less comparable.

For the long crystal sides (Figs. 1*b* and *c*), again three geometries are possible, which are also visualized in Fig. 11 (sides *F*, *G* and *H*). Crystal side *H* is completely built up by {111} faces. Adatoms will be preferentially incorporated in the re-entrant groove because they will have four neighbouring atoms there. After these atoms are incorporated, step and kink sites will be formed. The steps on these {111} faces will also increase the growth rate of the {111} adjacent faces. The preferential lateral growth of this side will be small because two-dimensional nucleation can only occur on one row of atoms. Side *H* was also prosposed by Maskasky (1987*a*). In his view, this side also occurs on the short side of triple twinned crystals. Sides *F* and *G* will express preferential lateral growth. For side *F*, the two {111} faces are linked with substeps to the {100} faces. This side was also proposed by Mehta, Jagannathan & Timmons (1993). Side-face structure *G* contains one {100} face, which is linked to two {111} faces with substeps. As we have already discussed, the $(\bar{1}11)'$ face will increase its growth rate owing to the substep mechanism.

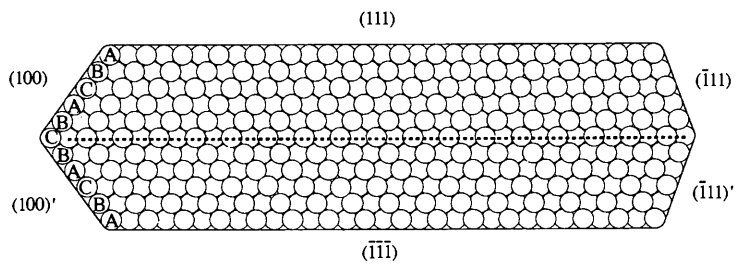

Fig. 9. Cubo-octahedral crystal with one twin plane parallel to the (111) face. The figure corresponds with the single twinned crystal in Fig. 5.

While our crystals have a long growth time, it is most likely that crystals with the fastest growing profiles occur because crystals with slower growing sides (like side *H*) have a greater chance of dissolving owing to the physical ripening process. Therefore, the crystal sides of groups 2 and 3 are probably built up by sides *C* and *D* (side *E* will transform to side *C*) for the short crystal sides and sides *F* and *G* for the long sides. The rate-determining step for the growth of sides *C*, *D* and *G* is the incorporation of an adatom at a position where it has four neighbours (on a {100} face and in the positions of the substep of 2/3).

However, when a critical nucleus has formed on a {100} surface, steps and kink sites emerge and a new growth layer is completed relatively quickly. Because of this, we assume that the formation of a nucleus is the rate-determining step in the growth process of a {100} face. The {100} faces adjacent to the tabular faces are much larger than the {100} faces between the twin planes. So the chance for a two-dimensional nucleus to form on these adjacent {100} faces is higher than on the {100} faces between the twin planes. Therefore, the growth rate of adjacent {100} faces is higher and sides *C* and *D* will express more preferential lateral growth than sides *F* and *G*. For side *F*, the rate-determining step is the two-dimensional nucleation process on two {100} faces, whereas for side *G* the rate-determining step is the two-dimensional nucleation process on only one {100} face and in a position of the substep of 2/3. Therefore, the growth rate of side *F* is expected to be somewhat larger. Thus, the triangular-shaped crystals will consist of the short crystal sides of sides *C* or *D* and on the long side they will contain side *G*. More intermediate shapes will have sides *C* and *D* on the short crystal side and side *F* on the long sides.

We applied the same side-face geometry to groups 2 and 3. For group 3, this is obvious because only two adjacent faces were determined. But for group 2, a face between two twin planes is also known. Therefore, it is surprising to find that all of the most probable crystal sides (*C*, *D*, *F* and *G*) fit also for the crystals of group 2. This leads to the conclusion that the crystals of groups 2 and 3 have the same side-face geometry. Only one twin plane (accidental twin plane) in group 2 was formed later.

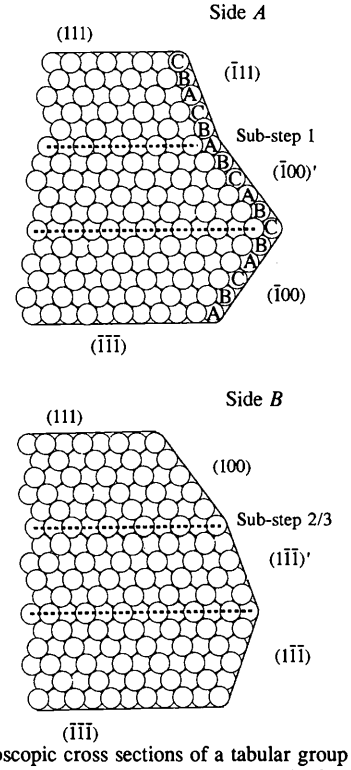

Fig. 10. Microscopic cross sections of a tabular group 1 crystal with two twin planes parallel to the tabular faces. The figure corresponds to the crystal in Fig. 1(*a*). Note that the distance between the twin planes is relatively exaggerated.

5. Relevance for industrial precipitation

The tabular crystals we discussed were grown under conditions optimized for ideal characterization. This means that the examined crystals were as large as possible with an aspect ratio between 4 and 60. With a change of the growth conditions, it was also possible to grow tabular crystals with different side-face structures. These side-face structures were examined (Millan & Bennema, 1997) using SEM. The crystal sides consisted of large {111} faces and sometimes small {100} faces were observed. Under these conditions, it is assumed that the {100} face is growing in a rougher mode. A rough growing face will tend to grow out of the crystal. In the case of silver bromide, this is only possible for {100} faces adjacent to the tabular faces. A {100} face adjacent to a tabular face will grow out leaving a {111} face behind that makes an acute edge with the top (or bottom) face.

Crystal side *A* (Fig. 10) can be transferred into the ridge/trough structure, first suggested by Hamilton & Brady (1964), or the rough–smooth structure, suggested by Mehta, Jagannathan & Timmons (1993), depending on whether the {100} plane between the twin planes is transferred into another plane or not. The {100} face adjacent to the tabular faces of sides *C*, *D* and *E* in Fig. 11 will be transferred into {111} faces. This leads to geometries with two acute edges. The adjacent side faces of sides *C*, *D* and *E* will of course not change when the {100} faces are growing as rough faces. So the group 1 crystals will develop side-face structures with one acute edge whereas the crystals of groups 2 and 3 will have two acute edges. The side-face structure of the tabular crystals grown by industry (precipitation in water) must be between two limits. When no rough growth on the {100} side faces occurs, the geometry will be the same as discussed in this paper, while rough growth of the {100} faces leads to geometries with

{111} side faces and for adjacent {100} faces to acute {111} lips. The situation in between will lead to structures with (small) {100} faces on the acute edges. Thus, the roughness of the {100} faces plays a key role in the side-face structure and therefore in the tabular morphology. The stability of the {100} face is determined by kinetic roughening depending on the applied supersaturation. In the early stages of precipitation, the {100} faces are probably rougher and acute lips are expected to be observed. In the physical ripening stage, the supersaturation is very low and the {100} becomes stable. In this situation, crystals obtain more ridge side-face structures as discussed in this paper.

6. Concluding remarks

The side-face structure of tabular silver bromide crystals has been determined. It was possible to examine the crystals directly while no additional processing after the growth was necessary. The side faces were established by using a goniometer and a SEM. It was found that all side faces were built up by flat {111} and {100} faces, giving three different groups of tabular crystal. From this knowledge, the number of twin planes could be deduced using the twinned cubo-octahedron model. The results are in agreement with measurements carried out by Hamilton & Brady (1964) and Maskasky (1987*a*).

The faces between twin planes were determined by the sphere model based on the theory of Ming. In the model, only the nearest-neighbour interactions were taken into account to explain the preferential lateral growth of the crystals. However, the simple sphere model proved to be a powerful tool in understanding the lateral growth of all silver bromide tabular crystals. We extend this model to also include twinned crystals with stable {100} faces.

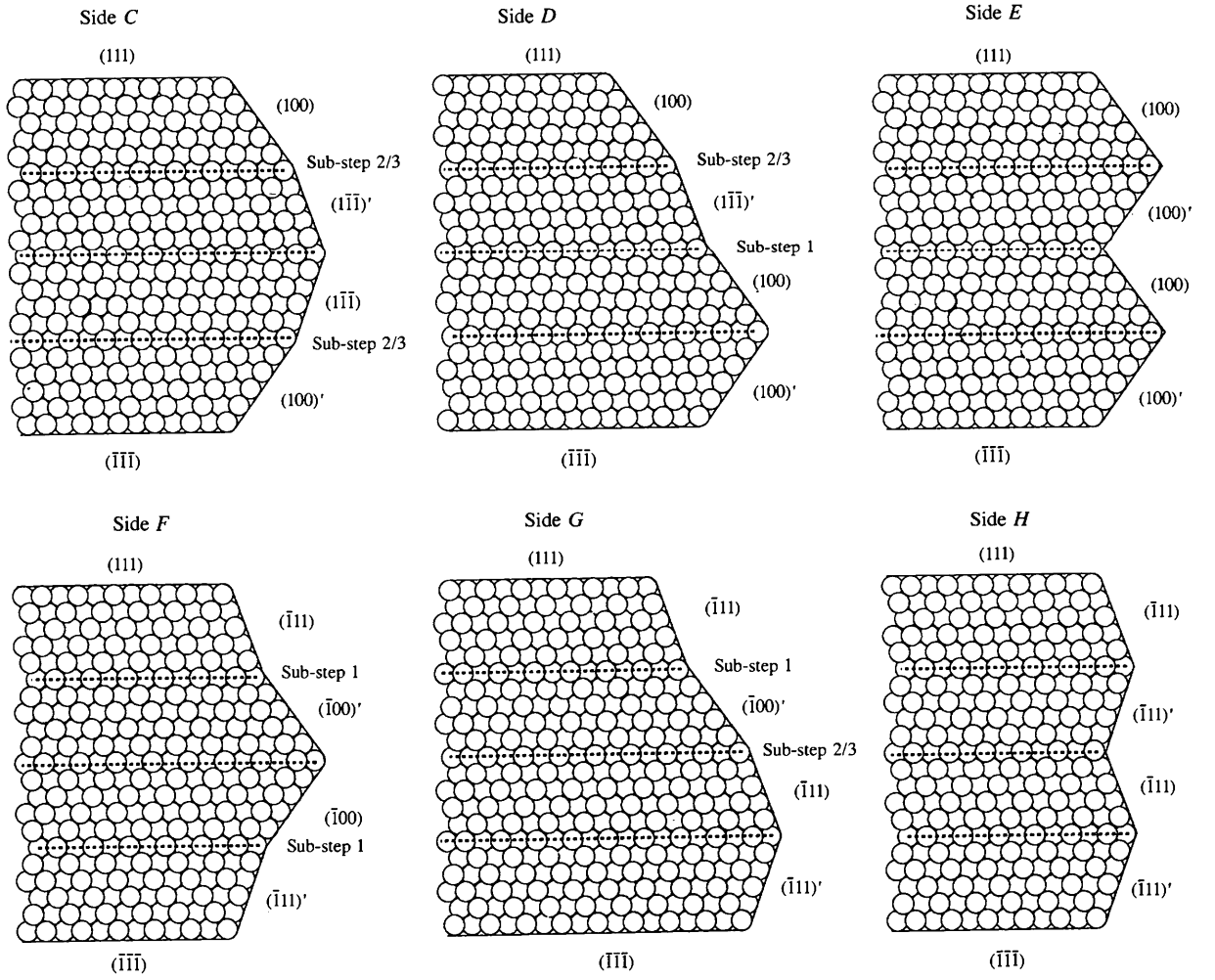

Fig. 11. Possible microscopic cross sections of a cubo-octahedral crystal with three twin planes parallel to the tabular faces. The figure corresponds to the crystal in Fig. 1(*c*).

For the double twinned tabular crystals of group 1, the side-face structure consists of two adjacent faces; one {111} face and one {100} face in a ridge structure. The face between the twin planes is a {111} or a {100} face. This results in two different side-face structures, both expressing preferential lateral growth owing to the substep mechanism. These side-face structures are assumed to have a somewhat different growth rate. Therefore, the occurrence of regular hexagonal and more intermediate shaped crystals is explained.

The side-face structure of the triple twinned groups 2 and 3 tabular crystals consists of two adjacent {111} faces on the long crystal side and two adjacent {100} faces on the short crystal side, both in a ridge structure. The faces between the twin planes are {111} and {100} faces, resulting in six different side-face structures. The four most probable structures expressing preferential lateral growth owing to the substep mechanism were established. The sides with two adjacent {100} faces are assumed to have a higher growth rate than sides with two adjacent {111} faces. Therefore, the occurrence of regular triangular and more intermediate shaped crystals is explained.

It turned out that the four most probable side-face structures fit not only for group 3 but also for group 2 crystals. This leads to the conclusion that the crystals of groups 2 and 3 have the same side-face geometry.

Future TEM measurements will be carried out in order to verify the number of twin planes of the different crystal groups. Moreover, work is in progress to explain why a simple sphere model works so well for explaining the tabular morphology of silver bromide.

References

Berriman, R. W. & Herz, R. H. (1957). *Nature (London)*, **180**, 293–294.

Farnell, G. C. & Judd, F. S. (1961). *J. Photogr. Sci.* **9**, 67–69.

Frank, F. C. (1949). *Discuss. Faraday Soc.* **5**, 48–58.

Hamilton, J. F. & Brady, L. E. (1958). *J. Appl. Phys.* **29**, 994.

Hamilton, J. F. & Brady, L. E. (1964), *J. Appl. Phys.* **35**, 414–421.

Jagannathan, R., Mehta, R. V., Timmons, J. A. & Black, D. L. (1993). *Phys. Rev. B*, **48**, 13261–13265.

Klein, E., Metz, H. J. & Moisar, E. (1963). *Photogr. Korresp.* **99**, 99.

Klein, E., Metz, H. J. & Moisar, E. (1964). *Mitteilungen aus den Forschungslaboratorien der Agfa-Gevaert AG Leverkusen*, Muchen Band IV. Berlin/Heidelberg/New York: Springer Verlag.

Maskasky, J. E. (1987*a*). *J. Imaging Sci.* **31**, 15–26.

Maskasky, J. E. (1987*b*). *J. Imaging Sci.* **31**, 93–99.

Mehta, R. V., Jagannathan, R., Lam, W. K., Black, D. L. & Timmons, J. A. (1995). *J. Imaging Sci. Technol.* **39**, 67–69.

Mehta, R. V., Jagannathan, R. & Timmons, J. A. (1993). *J. Imaging Sci. Technol.* **37**, 107–116.

Mehta, R. V., Jagannathan, R. & Timmons, J. A. (1996). *J. Imaging Sci. Technol.* **40**, 77–78.

Millan, A. & Bennema, P. (1997). In preparation.

Ming, N. (1993). *J. Cryst. Growth*, **128**, 104–112.

Ming, N. & Li, H. (1991). *J. Cryst. Growth*, **115**, 199–202.

Ming, N. & Sunagawa, I. (1988). *J. Cryst. Growth*, **87**, 13–17.

Mitchell, J. W. (1957). *Rep. Progr. Phys.* **22**, 433.

Sugimoto, T. (1984). *Photogr. Sci. Eng.* **28**, 137–145.

Waal, B. W. van de (1995). *Phys. Rev. B*, **51**, 8653.